CZECH TECHNICAL UNIVERSITY IN PRAGUE

FACULTY
OF MECHANICAL
ENGINEERING

SUMMARY OF DISSERTATION

CZECH TECHNICAL UNIVERSITY IN PRAGUE

Faculty of Mechanical Engineering

DEPARTMENT OF ENERGY ENGINEERING

Summary of Dissertation Thesis

Advanced Coatings of Nuclear Fuel Cladding

Jan Škarohlíd

Doctoral Study Program: Mechanical Engineering

Study Field: Power Engineering

Supervisor: *Doc. Ing. Radek Škoda*

Dissertation thesis statement for obtaining the academic title of "Doctor" abbreviated to "Ph.D."

Prague   *September, 2018*

Title in Czech language: *Pokročilé povlaky jaderného paliva*

This doctoral thesis is an outcome of a full-time doctoral study program at the Department of Power Engineering, Faculty of Mechanical Engineering, Czech Technical University in Prague.

Disertant: *Ing. Jan Škarohlíd*
    Department of Energy Engineering, Faculty of Mechanical Engineering, Czech Technical University in Prague
    Technická 4, 166 07 Praha 6

Supervisor: *Doc. Ing. Radek Škoda, Ph.D.*
    Department of Energy Engineering, Faculty of Mechanical Engineering, Czech Technical University in Prague
    Technická 4, 166 07 Praha 6

Supervisor Specialist: *Doc. Ing. Irena Kratochvílová, PhD*
    Institute of Physics, Czech Academy of Sciences
    Na Slovance 1999/2, 182 21 Praha 8

Reviewers:

Prof. Dr. Ing. Martin Vrňata, VŠCHT
doc. RNDr Přemysl Málek, CSc., MFF UK
doc. Ing. Luděk Jelínek, PhD, VŠCHT

The thesis was set out on:

The defense of the dissertation thesis will take place on:
Faculty of Mechanical Engineering, CTU in Prague, Technická 4, Praha 6 - Dejvice.

The thesis is available in the Department od Science and Research of Faculty of Mechanical Engineering, CTU in Prague, Technická 4, Praha 6 - Dejvice.

Prof. Ing. František Hrdlička, CSc.
Head of Doctoral Study Field Power Engineering
Faculty of Mechanical Engineering CTU in Prague

Název práce: *Pokročilé povlaky jaderného paliva*

Anotace:

Tato práce se zabývá ochranou zirkoniového (Zr) pokrytí jaderného paliva proti korozi a vysokoteplotní ve vodou chlazených jaderných reaktorech (LWR) povlaky polykrystalického diamantu (PCD) nebo směsného nitridu chromu, hliníku a křemíku (CrAlSiN). Bylo prokázáno, že povrchy slitin Zr mohou být účinně chráněny proti oxidaci při havarijních a pracovních teplotách v LWR pokrytím povrchu zirkonia vrstvou PCD nebo CrAlSiN. Každý povlak funguje specifickým způsobem a pro konkrétní účel.

PCD (300-700 nm) vrstva se skládá ze dvou různých uhlíkových fází: diamant a sp^2 uhlík účinně snižuje korozi Zr při provozní teplotě (o cca 40 %). Kromě zabránění přímému kontaktu Zr slitin s vodou, resp. párou, uhlík uvolněný z PCD filmu vstupuje a mění fyzikální vlastnosti podkladového povrchu Zr slitiny.

Povlaky CrAlSiN mají tloušťku 2 až 4,5 μm a slouží jako plná bariéra proti difúzi kyslíku při vysoké teplotě páry kolem 1000 °C, silně v závislosti na nepřítomnosti mechanických defektů.

Title: *Advanced Coatings of Nuclear Fuel Cladding*

Abstract:

This thesis deals with the protection of zirconium (Zr) nuclear fuel cladding against corrosion and high-temperature oxidation in water-cooled nuclear reactors (LWR) with coatings of polycrystalline diamond (PCD) or mixed nitride of chromium, aluminium and silicon (CrAlSiN). It has been shown that Zr alloy surfaces can be effectively protected against oxidation at accidental and operating temperatures in the LWR by coating the zirconium surface with a PCD or CrAlSiN layer. Each coating works in a specific way and for a particular purpose.

The PCD (300-700 nm) layer consists of two different carbon phases: diamond and sp^2 carbon and effectively reduces Zr corrosion at operating temperature (about 40%). In addition to avoiding the direct contact of Zr with water or steam, the carbon released from the PCD film enters and changes the physical properties of the Zr alloy substrate surface.

CrAlSiN coatings have a thickness of 2 to 4.5 μm and serve as a full barrier against oxygen diffusion at a high steam temperature of about 1000 °C, strongly depending on the absence of mechanical defects.

1. ***Contents***

2. Current status of Research

Currently, zirconium (Zr) alloys are used in all commercially operated power light-water (PWR, BWR and VVER) and heavy-water (CANDU) nuclear reactors. Zr alloys are used as a construction material for fuel cladding and other structural elements as fuel assemblies and core internals [3]. The main reason for their use is the low parasitic absorption of neutrons and high radiation resistance, good mechanical, thermal and chemical stability.

Zirconium alloys are it's use is accompanied with several negative aspects and processes as Pellet Cladding Interaction, Irradiation Assisted Stress Corrosion Cracking, Hydrogen Uptake (HU) leading to Delayed Hydride Cracking, and High-temperature Oxidation (HTO) [2], [4], [5].

High-temperature oxidation is strongly exothermic reaction between zirconium and water, which occurs at temperatures above 800 °C. [6]. Hydrogen and considerable amount of heat is released during this reaction. Degradation of the cladding tube will lead to the contamination of primary circuit with radiotoxic isotopes of nuclear fuel, fission products and transuranics, and potential radioactivity release. Arisen hydrogen, which as a combustible gas, impose a serious risk in the case of a severe accident conditions [7]. Released heat will strongly contribute to the potential core melting [A1].

As nuclear accidents with core temperatures higher than 800 °C are highly unlikely, the potential coating should be not only safety benefit but economical and plant operational benefit too. So, aim of this work is not only look for Zr alloy surface modifications, which could be beneficial at temperatures above 800 °C (Accident Tolerant Fuel – ATF), but also on materials and their performance at operational conditions at lower

8

temperatures 300 – 400 °C [12], [13]. Specially, this work deals with a protection of zirconium (Zr) nuclear fuel cladding material against corrosion in water-cooled nuclear reactors by coating of polycrystalline diamond (PCD) or chromium-aluminum-silicon nitrate layers (CrAlSiN).

Hence fuel cladding is one on most important barriers keeping radioactive and radiotoxic material separated from cooling water is necessary to operate not only in conditions that occur regularly in normal operation (Cat. 1. with frequency ~ 10) and during faults that are expected during the life of the power plant, and which requires safety response (Cat 2. with frequency ~1). Even more, fuel cladding has to withstand conditions caused by faults which are not expected during a life of a particular plant (Cat 3. with occurrence ~10^{-2}) and as the design considered conditions are taken improbable events, which are not expected to occur in nuclear industry (Cat. 4. with probability ~10^{-4}).

Typical temperatures for cladding and fuel LOCA cladding temperature transient is on.Fig. 1
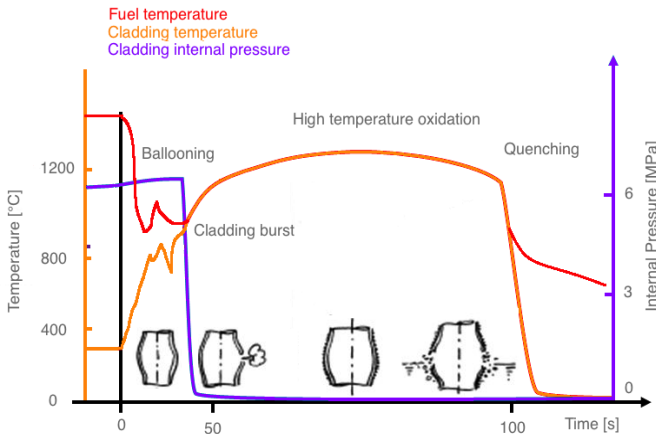

Fig. 1: Typical LOCA temperature transient

9

Several zirconium alloys were developed and slightly which differ in alloying elements concentration. We can distinguish between sponge-based alloys (e.g. Zr1Nb by Russian TVEL) and non-sponge-based alloys (e.g. Zirlo by Westinghouse, M5 by Areva). Sponge based alloys contain high concentration of niobium, non-sponge alloys are niobium free (except M5, where alloying niobium is added artificially. In this work Zirlo and Zircaloy-2 was used, as they were kindly provided by Westinghouse.

Below 865 °C, pure Zr has an hcp (hexagonal close packing) structure, with a c/a ratio of 1,593. The lattice parameters are a. 0,323 nm and c. 0,515nm (Zr α phase). At 865 °C, Zr undergoes an allotropic transformation from the low temperature hcp α phase to the high temperature bcc (body centered cubic) β phase. On cooling, the transformation is usually bainitic. The melting temperature of pure Zr is 1860 °C [1].

Protective coatings on Zr cladding tubes

One way how to protect Zr nuclear fuel cladding material against corrosion in water-cooled nuclear reactors is coating Zr nuclear fuel cladding surface by polycrystalline diamond and chromium-aluminum-silicon nitrate layers.

Layer thickness is one of the most important technological coating properties. Optimal thickness usually balances between thick robust layer with thickness in tens of micrometers providing adequate protection against oxygen and hydrogen but with higher tendency to cracking and peeling and thin layers (with thickness in hundreds of nanometers), which provides less

protection but have much better layer adhesively with low tendency to peeling.

Layer adhesivity is complex phenomena combining several properties and effects. Generally, with increase of the coating thickness the difference between Young's modulus is more significant and the coating is less able to compensate hoop stress of the cladding. This effect leads to cracking and peeling of the coating.

Protective coating of zirconium fuel cladding should provide additional time by delaying heat released from zirconium oxidation, this time could allow ECCS to handle the coolant loss in the core sooner, without start of cladding oxidation. Some preliminary analyses [9], [10], [23] shows that even delay in tens of minutes before breakaway oxidation can have significant impact on work of ECCSs.

Both these situations are DBA or post DBA with probabilities around $10^{-4} - 10^{-6}$, thus is more than reasonable to look for other advantages, which will not only increase safety but also bring some benefits for vendors, fuel manufacturers and plant operators. These benefits can be: decreasing cladding surface oxidation and hydrogen uptake, lower CRUD formation, higher fretting resistance, benefits to heat transfer and neutron moderation / absorption, longer lifetime of nuclear cladding and consequently enhancing nuclear fuel burnup.

3. *Thesis tasks and goals*

Main thesis goals were:

1. Preparation of coated samples, which involved these tasks:

o *selection of candidate coatings, with perspective properties and suitable methods for coatings deployment and acquisition of suitable substrate material – zirconium alloy*

o *preliminary testing of coated cladding samples (optical appearance after high temperature, adhesion of coatings)*

2. Exposure to conditions simulating conditions during LOCA

o *experimental setup for simulation of LOCA conditions*

o *preparation of exposed coated samples at operation a LOCA conditions.*

3. Evaluation of exposed samples using enhanced analytical methods and description of anticorrosive principles.

During first goal substrate materials were kindly provided by Westinghouse Electric. Two best candidates were CrAlSiN and PCD. Special experimental setup was built to test coated samples in steam environment at high temperatures.

In order to get more precise data long-term exposures (simulating reactor operation conditions) were performed in Westinghouse's laboratories in Pittsburgh, as there are no other suitable and available facilities. High-temp exposures and thermogravimetry were realized in Karlsruhe Institute of Technology during scientific internship.

4. Instrumentation and methods

PELAM CVD – preparation of PCD coatings

Samples of fuel cladding tubes and plates were immersed in a colloidal solution of diamond nanoparticles. The diamond nanoparticles acted as seeds and therefore as nucleation sites for PCD layer growth. Each Zr alloy sample was then coated with a homogeneous PCD layer grown using an MW-LA-PECVD apparatus [30]. PCD layers of 200-300 nm (labeled as 300 nm), 400-500 nm (labeled as 500 nm) and 600-700 nm (labeled as 700 nm) were produced [A3], [A2].

We presume that inner surface of tubular samples was coated only partly. This was considered during cross-section microscopic evaluations and oxide thickness measurements, where all cross-sections were edges of exposed samples were brushed out and samples were polished at it's middle sections.

Physical Vapor Deposition (PVD) – preparation of CrAlSiN coatings

CrAlSiN was deposited on Zircaloy-2 zirconium alloy using standard commercially available method of Physical Vapor Deposition (PVD). Composition of nitrides in coating is: 36,5 % (Al), 4,8 % (Si), 58,7 (Cr). Thickens of the coating varies between 2 – 4,5 μm. Samples were coated only on outer surface.

Long-Term Exposure in Reactor Operation Conditions

To simulate the long-term protective capabilities of both coatings under normal conditions in a nuclear reactor, PCD-coated and reference uncoated samples were subjected to a

series of high-temperature autoclave water tests. In accordance with ASTM standard procedures [31], the samples were exposed for 3 and 6 days in hot steam environment (400 °C and 11,6 MPa) and 6, 15, 20, 30, 40, 90, 120, 150, 170 and 195 days in hot water (360 °C, 16 MPa), close to the conditions found in the primary circuit of a PWR. Exposures in steam were performed at VSCHT laboratories and water exposures at the Westinghouse facilities in Pittsburgh, USA. No additional chemicals were used in both tests.

Thermogravimetry (TG)

TG measurements were performed at temperatures between 900 and 1100 °C in a NETZSCH thermobalance (model STA 409). Argon was used as an inert cover gas. Steam exposures were performed isothermally, without any changes in the steam (3 g per hour) or cover gas (3 l per hour) flow rates. The overall weight gain (w_g) was determined by measuring the sample's weight before and after oxidation. This weight was normalized with respect to the total exposed surface area of the sample to compensate for different sample sizes.

Off-gas analysis

Outgoing gas analysis was performed with a Balzers GAM 300 quadrupole mass spectrometer during high-temperature exposures.

Ion Beam Irradiation

To achieve a damage level of 10 dpp, the samples were irradiated by 3 MeV Fe^+ ions to a fluency of $1{,}95 \times 10^{16}$ cm^{-2}.. The irradiation was performed at room temperature. The projected range of Fe^+ ions is about 1,1 µm and the coating thickness is about 300 nm. Therefore Fe^+ ion penetration is deep enough to pass through the coating/substate interface.

5. *Results and discussion*

PCD Long-Term Exposure in Reactor Operation Conditions

Specimens were tested for a maximum of 195 days with specimen weight gains obtained at intermediate times and upon completion of the tests [A2]. In Fig. 2 are displayed weight gains measured after long term exposure in water environment of PCD coated Zr samples and uncoated reference Zr samples, in all cases the PCD coated Zr samples have a lower weight gain than uncoated samples. Similar results were observed after exposure in steam environment (400 °C) for 4 days. In this case the weight gain for a 300 nm PCD layer coated Zr sample was 7,8 $mg.dm^{-2}$, whereas the weight gain for an uncoated Zr sample was 13,2 $mg.dm^{-2}$.
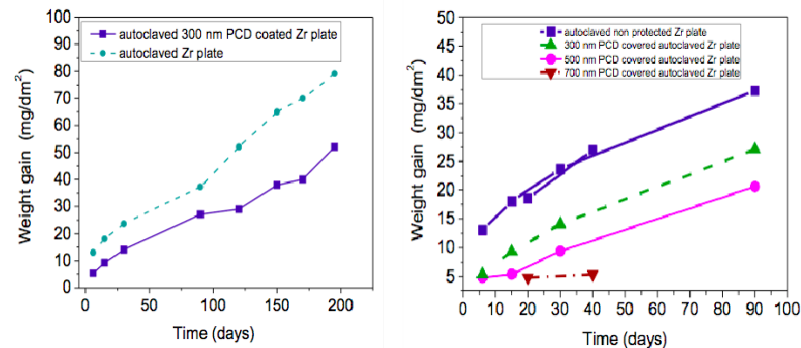
F i g . 2: (left) weight gains (mg.dm⁻²) after exposure in water environment (360 °C)

Tube samples and strip samples are from different materials, while tubular samples are form Zirlo and strip samples were low tin Zirlo. Only partial coverage with PCD layer is expected at inner surface of tubular samples.

PCD Ion Beam Irradiation

After the Ion Irradiation test the Raman spectra of the PCD film showed an increase in the intensity of the graphite related peak ($\sim$1600 cm⁻¹) and the diamond film still shows satisfactory structural integrity with both sp^3 and sp^2 carbon phases. This can be the effect of sp^3 carbon chemical bounds breaking and conversion into sp^2 carbon as inclusions in film due displacement of carbon atoms. Scanning Electron Microscopy was employed to evaluate coverage, crystal size, crystal shape and growth rates on all grown layers. Coverage of seeded areas was found to be with no pinholes for all layers. No change in the

16

polycrystalline diamond layer after ion beam irradiation was detected [A5].

PCD Thermogravimetry and hydrogen production measurement

Weight gain time dependences of PCD coated samples, measured by NETZCH thermo-balance at different temperatures from 900 °C to 1200 °C are on Fig. 3 and hydrogen concentration outgoing gas is on Fig. 4.
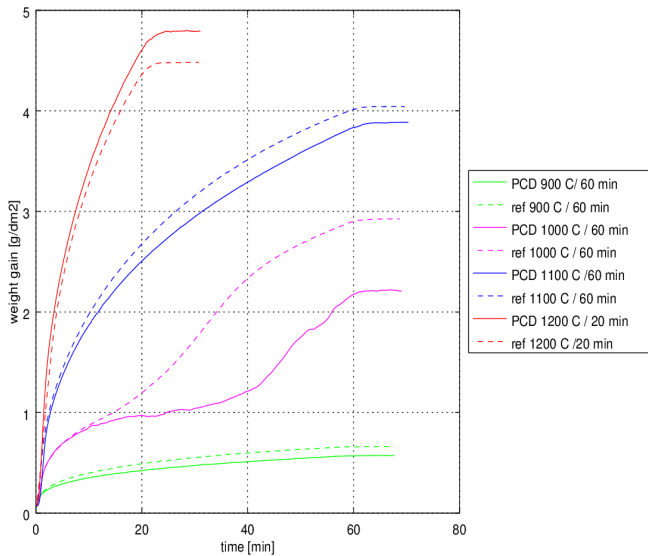

Fig. 3: Thermogravimetry of PCD coated Zirlo

Oxidation kinetics of PCD coated samples is similar to kinetics of uncoated samples at almost all temperatures, but with lower hydrogen production and lower weight gains. Most important difference is in later beginning of breakaway oxidation at

1000 °C, when breakaway oxidation starts on PCD coated sample 15 minutes later.
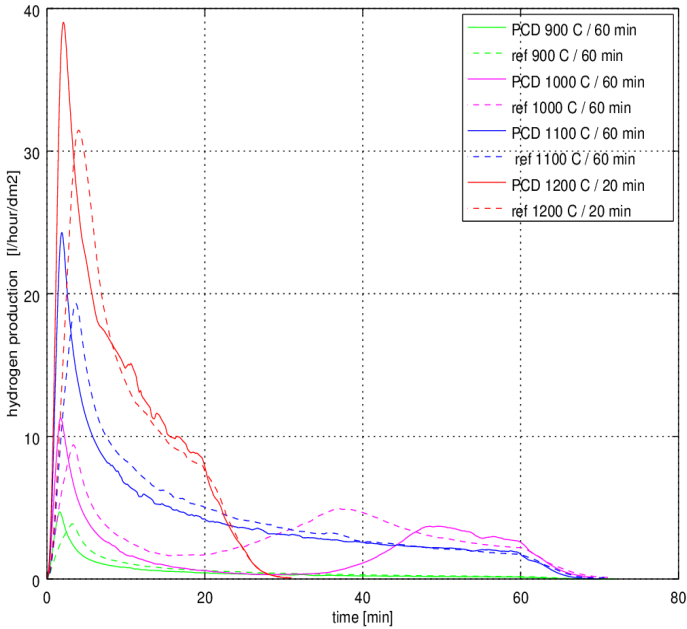

Fig. 4: Hydrogen production during TG exposures of PCD coated Zirlo

Special test with sample pre-oxidation was performed in order to see any changes (if they occur) in structure of PCD layer at temperatures below 800 °C. Pre-oxidation phase at 500 °C and 700 °C for 20 minutes was chosen, before exposing the sample to steam at 1000 °C. No steam was introduced to the furnace during transition heating phases. Sample with higher (700 °C) temperature of pre-oxidation phase has lower weight gain and hydrogen release in main oxidation phase, what is probably

caused by thicker oxide layer developed during pre-oxidation phase. No failure of PCD layer was observed during pre-oxidation phase [A6].

PCD Raman spectroscopy

Raman spectroscopy was performed on all tube samples coated with polycrystalline diamond (PCD) film prior and after each testing (Long-term corrosion testing, high temperature oxidation tests and Ion beam irradiation) to gain insight on diamond layer changes during oxidation. All measurements were carried out at room temperature using a Renishaw InVia Raman Microscope.

Raman spectroscopy measurements on the PCD coated samples before testing exposures revealed the existence of peaks related to sp^3 diamond (1332 cm^{-1}) and sp^2 – containing graphitic carbon (1600 cm^{-1}) phases. Measurements taken at positions over the entire surface of the cladding tube showed diamond
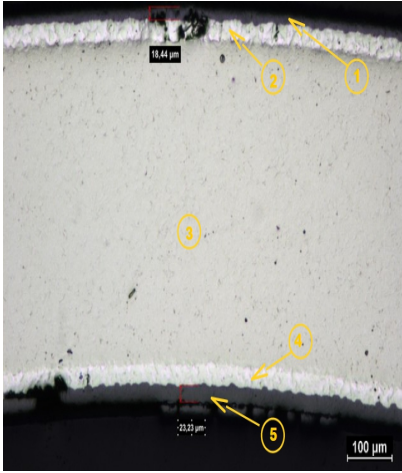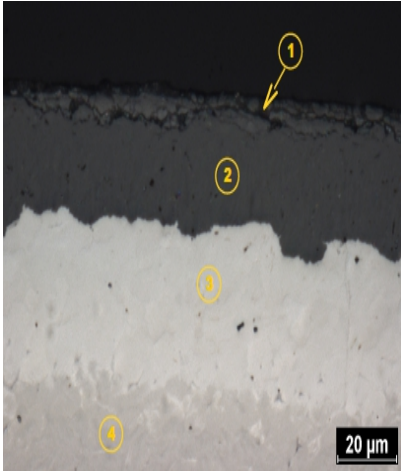
growth and incorporation of amorphous carbon and graphite.

No change in PCD layer was observed after long-term exposure (Fig. 5). After oxidation at 900 °C, 1000 °C and 1100 °C a mixture of sp^2 carbon, sp^3 carbon (diamond) and graphite-related features are visible. At 1200 °C steam exposed sample a complete transition to the graphite-related content is evident by a narrowing of the peak widths. A weak signal sample at 1400 °C suggests the rapid transition of the diamond coating to various carbon phases.

PCD Optical microscopy

Different polishing and etching techniques were used for sample preparations, that resulted in slightly different look of metalographs. Furthermore, different types of metallographical microscopes at different laboratories (KIT, CTU) were used, so enlightening is also different. Cross-section metallographic results are discussed in Table 1.

Table 1: PCD coated samples after 900 °C / 60 minutes exposure

PCD (Zirlo) – 900 °C, 60 min

- **Outer oxide thickness: 18,44 µm**
- **Inner oxide thickness: 23,23 µm**

Optical microscopy reveals oxide grows below PCD layer on outer surface. Oxidation rate is lower on the outer tube surface

which was protected by thin PCD layer, then on the inner unprotected surface.

PCD Hydrogen concentration in Zr metal measured by IGF

The samples were taken from the center of each piece to avoid edge effects. The PCD coating was not removed prior to the analysis. Knowing the area, initial weight and final weight of each sample, along with the bulk hydrogen concentration, the hydrogen pickup fraction was calculated. The initial hydrogen concentration of 8 ppm was used in the hydrogen pickup calculations. Measured values are summarized in Table 2.

Table 2: Hydrogen concentrations measured by IGF [A2]

Temp.	Time	Hydrogen concentration	
[°C]	[min]	[ppm]	
		Coated	Reference
PCD coatings on Zirlo			
1200	2 x 30	63,35	520,8
1100	60	51,33	571,4
400	3 days	25,6	17,8
PCD on Zry-2			
1200	2x30	69,17	62,3
PCD on low Sn Zr			
400	3 days	21,85	16,6

PCD X-ray photoelectron spectroscopy

The protective capabilities of the PCD layers were further evidenced by XPS data acquired from the PCD-coated (300 nm)

and uncoated Zirlo tubes before and after steam exposure (in an autoclave for 4 days at 400 °C). The XPS spectra were obtained from cross sections of the samples.

Regarding the analysis of the carbon states, the presence of carbides and forms of carbon with a binding energy near 285 eV was determined from the detailed spectra of the C1s peak (Fig. 5).
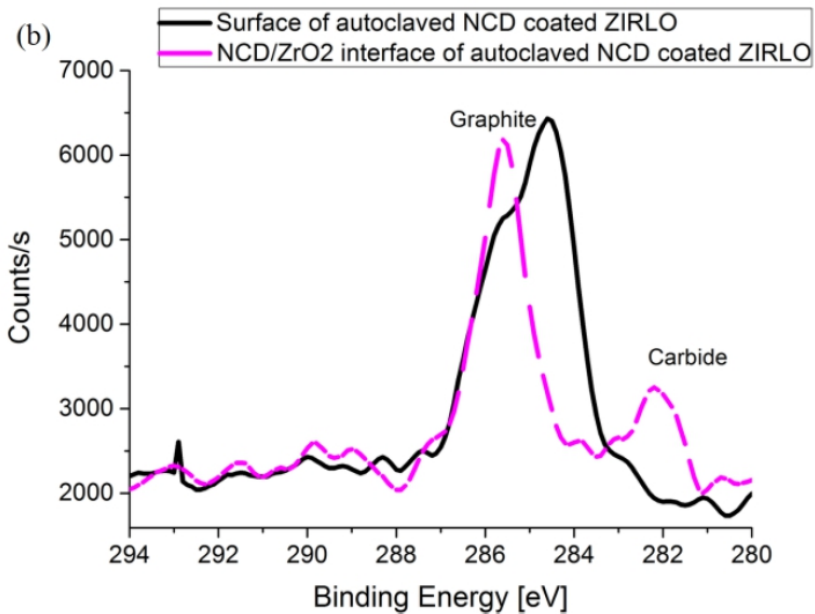

Fig. 5: XPS revealing presence of carbides on coating-substrate interface

PCD Secondary ion mass spectrometry (SIMS)

We used SIMS to determine the changes in the C depth profile of a 300 nm PCD-coated Zr alloy tube before and after 4 days of exposure to 400 °C hot steam. The SIMS data showed that after 4 days at 400 °C in hot steam, a large amount of C was contained in the ZrO2 layer formed beneath the protective PCD layer. The exposure to hot steam clearly resulted in the diffusion of carbon into the ZrO2 layer to a depth larger than 1,5 µm (Fig. 6). In a reference PCD-coated Zr alloy sample (not exposed to hot steam), the majority of the carbon atoms were contained within the thickness of the PCD layer itself. The depth profiles of C and O are in units of counts/s and labelled in the graphs.
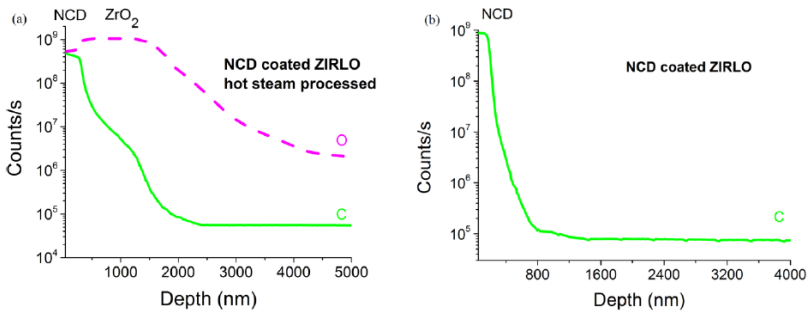

Fig. 6: SIMS data showing diffusion of carbon in Zr substrate

PCD Capacitance measurements

Capacitance measurements were performed on uncoated Zr alloy tubes before and after steam exposure (400 °C for 4 days) and on 300nm PCD-coated Zr alloy sample exposed to the same steam conditions. The types and densities of the defects in the surface films were determined.

Measurements showed, that the oxide films on uncoated and steam exposed samples were found to exhibit solely n-type semi-conductive behavior. This result was consistent with observations of pure zirconium [32] and of Zr-Nb and Zr-Sn alloys. The results of the doping density analysis are presented in Table 5, where N_A and N_D denote the acceptor and donor densities, respectively. A high donor density (characteristic of an n-type semiconductor) was found for the uncoated Zr samples both before and after hot steam exposure, whereas the PCD-coated Zr samples after steam exposure showed both p-type (acceptor-containing) and n-type semi-conductive behaviour (Table 3).

Table 3: Acceptor and donor densities obtained from the Mott-Schottky plots [A2]

Sample	$N_A [\mathrm{cm}^{-3}]$	$N_D [\mathrm{cm}^{-3}]$
Zirlo (uncoated)	-	4×10^{20}
Zirlo (4 days at 400 °C)	-	$2{,}3 \times 10^{18}$
Zirlo with 300 nm PCD, 4 days at 400 °C	$4{,}4 \times 10^{16}$	$2 - 3 \times 10^{16}$

CrAlSiN coating preparation

CrAlSiN was deposited on Zircaloy-2 zirconium alloy using method of Physical Vapor Deposition (PVD). Composition of nitrides in coating is: 36,5 % (Al), 4,8 % (Si), 58,7 (Cr). Thickens of the coating varies between 2 – 4,5 μm. As proved later samples were coated only on outer surface. Properties of prepared coating: Micro-hardness 35 GPa, thickness 2 – 4,5 μm and roughness Ra 0,15 – 0,20 μm.

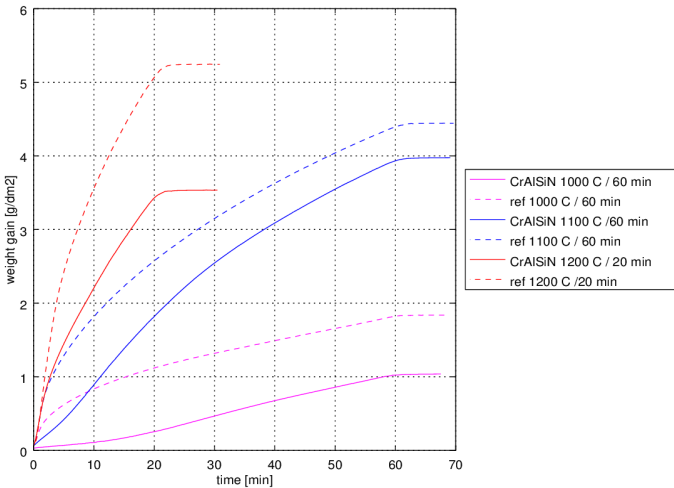**CrAlSiN Thermogravimetry and hydrogen production measurement**

Fig. 7: Thermogravimetry of CrAlSiN coated Zry-2

Weight gain and hydrogen production of CrAlSiN coated and reference samples are visualized in Fig. 7 and Fig. 8. Lower

hydrogen production and lower mass gain of CrAlSiN coated sample is visible at temperature 1000 °C.

Even at temperature 1100 °C is no hydrogen peak present at the beginning of steam exposure and also weight gain denotes lower reaction kinetics. Exposure at 1200 °C also shows lower oxidation kinetics but hydrogen peak during beginning of oxidations phase is present.
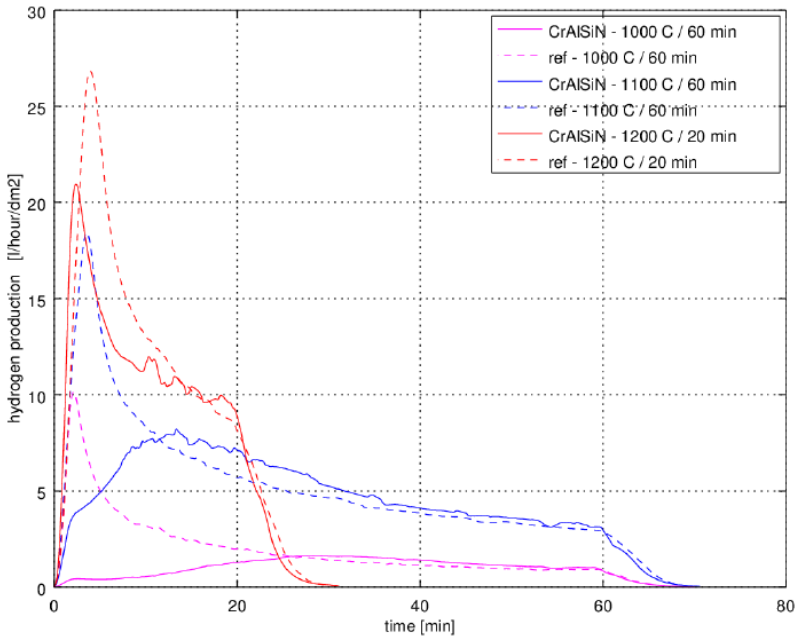

Fig. 8: Hydrogen production during TG exposures of CrAlSiN coated Zy-2

CrAlSiN High-temperature exposures

After first 30 minutes in steam were samples cooled down in inert argon atmosphere and removed from BOX furnace. Sample was then returned back to furnace after measuring of weight gain for second 30 minutes long exposure.

Very high temperature test was performed in BOX furnace. Exposition parameters were set as follows: temperature – 1400 °C, time – 6 min., argon flow-rate – 30 l/hour, steam flow-rate – 40 g/hour. Time was determined after previous calculation using Carthcarth – Pawel correlation in order to avoid complete oxidation of the sample. Data are summarized in Table 4.

Table 4: Overall weight gains and hydrogen productions from high temperature exposures

Temp.	Time	Weight gain		ECR		Hydrogen produced	
[°C]	[min]	$[g.dm^{-2}]$		[%]		$[l.dm^{-2}]$	
		Coated	Ref.	Coated	Ref.	Coated	Ref.
CrAlSiN coatings on Zry-2							
900	240	0,71	0,96	10,1	13,0	0,95	1,34
1000	60	1,38	0,98	19,7	13,9	1,57	1,26
1100	40	2,43	2,98	34,7	43,54	3,29	3,82
1200**	30	2,83	3,56	40,2	50,8	-na-	-na-
1200**	60	4,75	5,48	68,9	78,3	6,63	7,42
1400	6	4,82	3,29	68,86	44,48		

CrAlSiN Optical microscopy

Several polishing and etching techniques was used for sample preparations, that resulted in slightly different look of metalographs.

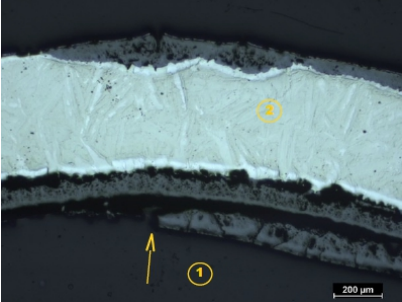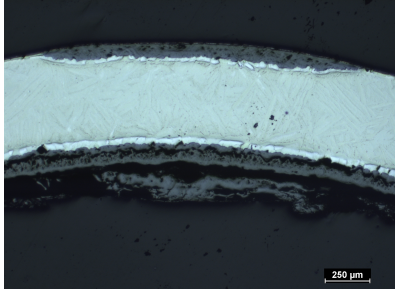*Table 5: CrAlSiN optical microscopy results at 1000 °C / 60 min. samples*

CrAlSiN (Zry-2) – 1000 °C, 60 min	
(1) Partial segregation of inner oxide layer – probably caused during polishing (2) Inner part of cladding tube still consist of relatively thick prior β-Zr phase	Several Zr oxide "nodes" or "blisters" with different size are present on outer surface.
• Inner oxide thickness: 230 μm • Outer (coated) surface oxide thickness (best): 0 μm • Outer (coated) surface oxide thickness (worst): 360 μm	

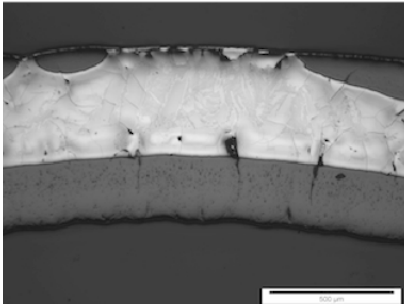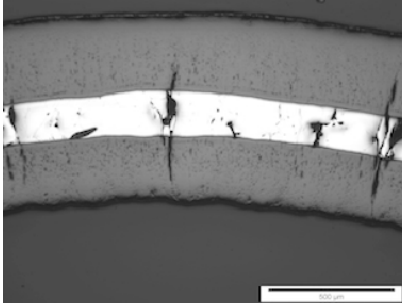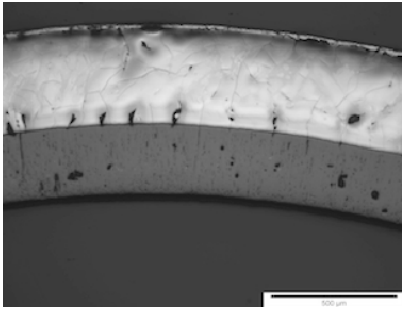*Table 6: CrAlSiN optical microscopy results at 1100 °C / 60 min. samples*

CrAlSiN – 1100 °C, 60 minutes

Several failures of coating on outer surface with developing oxide layer with variable thickness. Thin α-Zr layer is visible on Zr oxide blisters on outer surface, but prior β-Zr is still present on significant part near outer surface.	Thick oxide layers on both outer and inner surfaces are visible. No prior β-Zr phase is present.

- **Inner oxide thickness: 230 µm**
- **Outer (coated) surface oxide thickness (best): 0 µm**
- **Outer (coated) surface oxide thickness (worst): 360 µm**

- **Reference sample inner oxide thickness: 260 µm**
- **Reference sample outer oxide thickness: 310 µm**

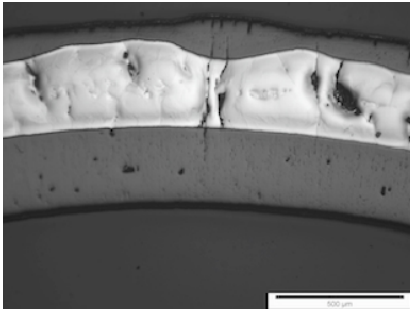*Table 7: CrAlSiN optical microscopy results at 1200 °C / 20 min. samples*

CrAlSiN – 1200 °C, 20 minutes	
Optical microscopy reveals no ZrO_2 layer on outer surface. No prior β-Zr phase on outer diameter indicates no or very limited diffusion of oxygen through the coating.	Thick oxide layer on inner surface and developing homogenous Zr oxide layer on outer surface with variable thickness are visible. No prior β-Zr phase is present.
- Inner oxide thickness: 290 μm - Outer (coated) surface oxide thickness (best): 0 μm - Outer (coated) surface oxide thickness (worst): 170 μm	
- Reference sample inner oxide thickness: 212 μm - Reference sample outer oxide thickness: 283 μm	

From metallographic observations (Table 5, Table 6, Table 7) is clear that CrAlSiN coated samples were coated only at the outer surface, what has strong influence on measured data, where mixed oxidation of coated and uncoated surface occurs. On the other hand at metallographic observation serves inner oxide

layer as a good reference in coated and uncoated surface's oxide layer thickness. Thickens of outer (coated) oxide layer varies from zero to same or even higher thickness then inner oxide. Fully protected and unprotected places (with most thick oxide) are randomly distributed along outer surfaces. At fully protected places is still apparent prior β-Zr structure. Prior β-Zr phase with no oxygen stabilized zirconium alpha phase indicates no, or very low oxygen diffusion through the CrAlSiN coating into the zirconium metal. Nodular (or "blister") pattern is quite common on outer surface and indicates places, where protective coating mechanical fails and steam starts to penetrate zirconium alloy through cracks in coating.

CrAlSiN Hydrogen concentration in Zr metal measured by IGF

Knowing the area, initial weight and final weight of each sample, along with the bulk hydrogen concentration, the hydrogen pickup fraction was calculated. The initial hydrogen concentration of 8 ppm was used in the hydrogen pickup calculations. Measured values are summarized in Table 8.

Table 8: Hydrogen concentrations measured by IGF

Temp.	Time	Hydrogen concentration	
[°C]	[min]	[ppm]	
		Coated	Reference
CrAlSin on Zry-2			
1200	2 x 30	141,4	62,3
1100	40	388,8	612,4
1000	60	1528,4	282,85

CrAlSiN EDS observations

As there is no nitrogen present in the formal CrAlSiN coating is obvious that all coating has been oxidized, replacing chromium, aluminium and silicon nitrides with chromium oxide, alumina and silica. Average ratio among Cr: Al : Si is 10 : 3,5 : 0,4 3 which roughly corresponds with initial ratio 58,7% (Cr), 36,5 % (Al) and 4,8 % (Si).

Spectrum measured just underneath the CrAlSiN coating, shows no, or very limited diffusion of coating element (Cr, Si, Al) into the underlying zirconium material.

6. *Conclusions*

After long-term processing (for up to 195 days) in 360 °C hot water (in accordance with ASTM standard procedures), a larger relative weight gain was found for Zr alloy samples with unprotected surfaces than for PCD-coated samples. The relative

weight gain of the PCD-coated samples was decreased by 35 – 55 %. PCD layers were also found to protect Zr alloy surfaces against hydrogen uptake: the average hydrogen concentration was markedly greater for uncoated samples. For high-temperature steam exposures (1100 °C, 1200 °C), the uptake of hydrogen into the unprotected material was an order of magnitude higher than that indicated by the hydrogen concentrations in the PCD-protected samples.

Thicker (700 nm and 500 nm) PCD layers provided stronger protection of ZIRLO plates and tubes against oxidation than thinner (300 nm) PCD layers. The higher protective efficacy achieved by the PCD coatings for plates compared with tubes was attributed to the inner surfaces of the tubes not being fully covered with PCD, whereas in the case of plates mounted vertically in the deposition chamber, all surfaces were covered with homogeneous PCD layers. This protection of PCD occurs at three basic levels:

(1) the PCD protects the Zr alloy surface from directly interacting with water molecules;

(2) carbon atoms penetrate into the Zr alloy from the PCD, thus creating carbides and becoming incorporated into ZrO_2, thereby making conditions less favourable for subsequent O and H uptake; and

(3) the carbon from the PCD changes the electrical properties of the ZrO_2 and creates less favourable conditions for Zr oxidation at the ZrO_2/Zr interface. The specific anticorrosion function of PCD coating of Zr

33

alloy prepared in MW-LA-PECVD apparatus was patented in [A4].

Major points concerning Zr alloys new anticorrosion strategy using PCD coating are:

o Zr alloys used as nuclear fuel cladding and other structural elements in nuclear reactors covered by compact and homogeneous PCD layers consisting of sp^3 and sp^2 carbon phases with a high crystalline diamond content and low roughness are strongly protected against corrosion in hot steam / hot water environment.

o After ion beam irradiation (10 dpa, 3 MeV Fe2^{+}) the diamond layer shows satisfactory structural integrity with both sp^3 and sp^2 carbon phases.

o Exposure of the PCD coated Zr alloy to hot steam (1100 °C, 30 min) caused the infusion of both oxygen and Zr substrate atoms into the protective layer. The protective layer has a constitution of Zr carbide and underwent a phase change from diamond to sp^2 phase carbon.

o After 1100 °C steam oxidation of PCD coated Zr alloy samples, zirconium atoms are incorporated into PCD layer – first fingerprints of zirconium carbide layer were forming.

o The Zr alloy under the PCD protective layer after high temperature steam oxidation differed from the original alloy material composition only very slightly (XPS), proving that the PCD coating increases the material resistance to high temperature oxidation.

o The larger weight gain of unprotected Zr fuel cladding can be attributed to the greater oxygen intake compared to PCD covered/protected Zr fuel cladding.

o In addition to the fact that PCD layers prevent the surface of Zr alloys from direct interaction with hot water, carbon released from the PCD film enters and changes the physical properties of the underlying Zr. **This effect plays significant role in PCD protective function.**

o Compared with Zr samples protected with 500 nm of PCD, the hydrogen concentration in the unprotected Zr samples was found to be larger by one order of magnitude after 1 hour at 1100 °C in autoclave.

CrAlSiN coatings is homogeneous one phase layer. Thickens of the CrAlSiN coating varies between 2 – 4,5 μm.

o CrAlSiN coated samples shows significant changes in oxidation curves – especially eliminates initial very kinetic initial oxidation phase and also overall hydrogen production and weight gain values are generally lower than for uncoated samples. CrAlSiN coating works very well at temperatures around 1000 °C, where they delayed breakaway oxidation.

o From optical microscopy is clear that CrAlSiN coating serves as full barrier against oxygen diffusion, until mechanical failure of the coating. But when the CrAlSiN coatings mechanically failed the oxidation process is even faster than in the case of unprotected samples.

o Oxidation of the primary chromium, aluminium and silicon nitrides has been detected, leading to creation of highly stable and high temperature resistant alumina and chromium oxide layers.

References

Author references

[A1] Škarohlíd, J., Škoda, R., Kazda, R., (2013). Problematics of high-temperature oxidation of zirconium (in czech). *Bezpečnost jaderné energie*, **21**(59), 298-301.

[A2] Škarohlíd, J. *et al.* Nanocrystalline diamond protects Zr cladding surface against oxygen and hydrogen uptake: Nuclear fuel durability enhancement. *Scientific Reports* **7,** 1–14 (2017).

[A3] Ashcheulov, P. *et al.* Thin polycrystalline diamond films protecting zirconium alloys surfaces : From technology to layer analysis and application in nuclear facilities. *Applied Surface Science* **359,** 621–628 (2015).

[A4] Škoda, R., Škarohlíd, J., Kratochvílová, I., Taylor, A., Fendrych, F. (2015) Layer protecting the surface of zirconium alloys used in nuclear reactors. PCT WO/2015/039636, Czech patent 305059.

[A5] Kratochvílová, I. *et al.* Nanosized polycrystalline diamond cladding for surface protection of zirconium nuclear fuel tubes. *Journal of Materials Processing Technology* **214,** 2600–2605 (2014).

[A6] Škarohlíd, J., Škoda, R. & Kratochvílová, I. High temperature oxidation of polycrystalline diamond coated zirconium alloy. *International Conference on Nuclear Engineering, Proceedings, ICONE* **5,** 1–4 (2016).

Other references

[1] 1. Allen, T. R., Konings, R. J. M. & Motta, A. T. Corrosion of Zirconium Alloys. in *Comprehensive Nuclear Materials* (2012). doi:10.1016/B978-0-08-056033-5.00063-X

[2] Steinbrück, M., Vér, N., & Grosse, M. Oxidation of advanced zirconium cladding alloys in steam at temperatures in the range of 600-1200 °C. *Oxidation of Metals* **76,** 215-232, (2011).

[3] Fuel Design Data, *Nuclear Engineering International*, September 2004

[4] Cox, B. Some thoughts on the mechanisms of in-reactor corrosion of zirconium alloys. *Journal of Nuclear Materials* **336,** 331–368, (2005).

[5] Brachet, J.Ch. (2015) High temperature oxidation and LOCA behaviour of Zr alloys: microstructural evolutions, consequences on the mechanical properties. *Institut national des sciences et techniques nucléaires.*

[6] Evaluation of Conditions for Hydrogen Induced Degradation of Zirconium Alloys during Fuel Operation and Storage, IAEA-TECDOC-1781

[7] Mitigation of Hydrogen Hazards in Severe Accidents in Nuclear Power Plants, IAEA-TECDOC-1661

[8] Hirano, M. *et al.* Insights from review and analysis of the Fukushima Dai-ichi accident. *Journal of Nuclear Science and Technology* **49,** 1-17, (2012).

[9] Terrani, K. A. Accident tolerant fuel cladding development: Promise, status, and challenges. *Journal of Nuclear Materials* **501,** 13–30, (2018).

[10] Zinkle, S. J., Terrani, K. A., Gehin, J. C., Ott, L. J. & Snead, L. L. Accident tolerant fuels for LWRs: A perspective. *Journal of Nuclear Materials* **448,** 374–379, (2014).

[11] Tang, C., Stueber, M., Seifert, H. J. & Steinbrueck, M. Protective coatings on zirconium-based alloys as accident-Tolerant fuel (ATF) claddings. *Corrosion Reviews* **35,** 141–165, (2017).

[12] Motta, A. T., Couet, A., & Comstock, R. J. Corrosion of Zirconium Alloys Used for Nuclear Fuel Cladding. *Annual Review of Materials Research,* **45,** 311-343, (2015).

[13] Corrosion of zirconium alloys in nuclear power plants, IAEA-TECDOC-684

[14] United States Nuclear Regulatory Commission. NUREG/CR-6967. Cladding Embrittlement During Postulated Loss-of-Coolant Accidents. (2008).

[15] Likhanskii, V. V, & Evdokimov, I. Review of theoretical conceptions on regimes of oxidation and hydrogen pickup in Zr-alloys 2 . Factors affecting corrosion regimes of zirconium alloys. *IAEA NCL Collection.*

[16] Baek, J. H. & Jeong, Y. H. Breakaway phenomenon of Zr-based alloys during a high-temperature oxidation. *Journal of Nuclear Materials* **372,** 152–159 (2008).

[17] Young, D. High Temperature Oxidation and Corrosion of Metals. *Elsevier Corrosion Series*

[18] Pawel, R. E., Cathcart, J. V., McKee, R. A. (1979) The Kinetics of Oxidation of Zircaloy-4 in Steam at High Temperatures. *J. Electrochem. Soc.* **126**, 1105-1111 (1979).

[19] Baker, L., Just, J. C. Studies of Metal-Water Reactions at High Temperatures; III. Experimental and Theoretical Studies of the Zirconium-Water Reaction, ANL-6548, (1962).

[20] Pshenichnikov, A. & Stuckert, J. Orientation relationships of delta hydrides in zirconium and Zircaloy-4. *International Conference on Nuclear Engineering, Proceedings, ICONE* (2016).

[21] Puls, M. P. Review of the thermodynamic basis for models of delayed hydride cracking rate in zirconium alloys. *Journal of Nuclear Materials,* **393,** 350-367, (2009).

[22] Couet, A., Motta, A. T., & Comstock, R. J. Hydrogen pickup measurements in zirconium alloys: Relation to oxidation kinetics. *Journal of Nuclear Materials,* **451**, 1-13, (2014).

[23] Bragg-Sitton, S., Development of advanced accident-tolerant fules for commercial LWRs. *Nuclear News*, **4,** 83–91, (2014).

[24] Brachet, J. C. *et al.* Behavior under LOCA conditions of Enhanced Accident Tolerant Chromium Coated Zircaloy-4 Claddings. *Top Fuel 2016 Proceedings* (2016).

[25] Sung, J. H. *et al.* Fretting damage of TiN coated zircaloy-4 tube. *Wear* **250,** 658–664, (2001).

[26] Pu, J.-C. *et al.* High-temperature oxidation behaviors of CVD diamond films. *Applied Surface Science*. **256**(3), 668-673, (2009).

[27] Mercs, D. *et al.* Mechanical and tribological properties of Cr-N and Cr-SI-N coatings reactively sputter deposited. *Surface and Coatings Technology* **200,** 403–407 (2005).

[28] Rafaja, D. *et al.* Microstructure development in Cr-Al-Si-N nanocomposites deposited by cathodic arc evaporation. *Surface and Coatings Technology* **201,** 2835–2843 (2006).

[29] Polcar, T. & Cavaleiro, A. High-temperature tribological properties of CrAlN, CrAlSiN and AlCrSiN coatings. *Surface and Coatings Technology* **206,** 1244–1251 (2011).

[30] Fendrych, F. *et al*. Growth and characterization of nanodiamond layers prepared using the plasma-enhanced linear antennas microwave CVD system. *Journal of Physics D: Applied Physics*. **43**(37), (2010)

[31] ASTM G2 / G2M – 06 Standard Test Method for Corrosion Testing of Products of Zirconium, Hafnium, and Their Alloys in Water at 680°F [360°C] or in Steam at 750°F [400°C].

[32] Chen, Y. *et al*. The electrochemistry of zirconium in aqueous solutions at elevated temperatures and pressures. *Journal of Nuclear Materials* **348,** 133-147 (2006).